

## BULLET GROUPS AS A TEST OF $\Lambda$ CDM

J. G. FERNÁNDEZ-TRINCADO<sup>1,2,3</sup>, J. E. FORERO-ROMERO<sup>1</sup> AND T. VERDUGO<sup>3</sup>

<sup>1</sup> Departamento de Física, Universidad de los Andes, Cra. 1 No. 18A-10, Edificio Ip, Bogotá, Colombia

<sup>2</sup> Institute Utinam, CNRS UMR6213, Université de Franche-Comté, OSU THETA de Franche-Comté-Bourgogne, Besançon, France

<sup>3</sup> Centro de Investigaciones de Astronomía, AP 264, Mérida 5101-A, Venezuela

Submitted for publication in ApJL

## ABSTRACT

We estimate the expected distribution of displacements between the two dominant dark matter peaks in halos within a mass range corresponding to galaxy groups. We find that the probability of finding a system similar with displacements of  $\sim 400 h^{-1}$ kpc is between 40% for  $z=0$  and 60% for  $z=1$  and  $\Lambda$ CDM standard model, which correspond to the observational constraint the object SL2S J08544-0121 that is a gravitational lens found in the SL2S and located at  $z=0.35$ . Given the larger abundance of groups with respect to clusters, finding multi-modal groups and baryonic-dark matter displacements.

*Subject headings:* cosmology: theory – dark matter

## 1. INTRODUCTION

The Bullet Cluster provided a new kind of observational evidence of the existence of dark matter. Quantifying the displacement between dark matter and the dominant baryonic component (hot X-ray emitting gas) has been used to test the CDM paradigm itself by quantifying the substructure velocity required to produce such displacement and also by estimating the expected abundance of such events in the Universe.

Since that time there are other observations of other Bullet-like systems [...].

Recently (Gastaldello et al. 2014) observed baryonic-DM displacement of  $124 \pm 20$  kpc in a group-like system with a total mass  $2.4 \pm 0.6 \times 10^{14} M_{\odot}$ . Systems of this mass are  $\sim 10$  times more massive than cluster systems in the mass range  $> 10^{15} h^{-1} M_{\odot}$ , this opens up the possibility of observationally finding bullet groups in a fair amount to impose constraints on  $\Lambda$ CDM. This greater abundance has to be weighted by the fraction of systems that present large displacements. Such study has been performed for clusters but not for lower mass systems.

In this Letter we present prediction for the abundance of group-like systems that might show a DM-baryon displacement. To this end we use a N-body cosmological simulation with such a resolution that allows us to identify multimodal dark matter clumps in the circular velocity range  $300 - 1000$  km s $^{-1}$ .

This paper is organized as the follows. In Section 2 we present the simulation and the halo catalogs used in this work. We continue in Section 3 with the geometry of the problem at hand and the measurements setup. Next in Section 4 we present our results to finish with a discussion and conclusion in Sections 7 and 8.

## 2. SIMULATION AND HALO CATALOGS

We use the Bolshoi Run, a cosmological DM only simulation over a cubic volume of 250 comoving  $h^{-1}$ Mpc on a side. The simulation uses the ART code to follow the evolution of a dark matter density field sampled with  $2048^3$  from  $z = 80$  to  $z = 0$  [...]. The cosmology used corresponds to the spatially flat concordance model with the following parameters: the density parameter for

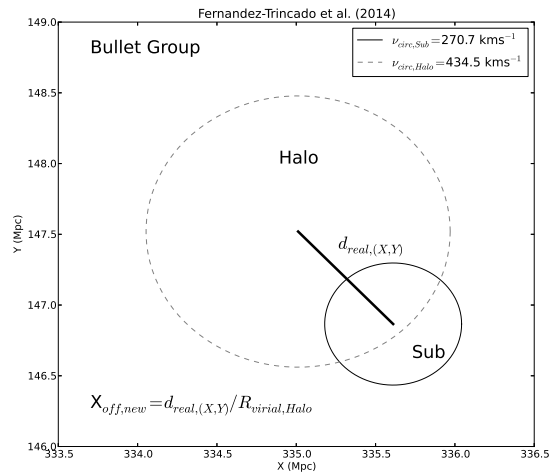


FIG. 1.— Configuration for a host halo (dashed circle) and substructure (black circle) in the sample.

matter (dark matter+baryons)  $\Omega_m = 0.27$ , the density parameter for baryonic matter  $\Omega_b = 0.0469$ , the density parameter for dark energy  $\Omega_\Lambda = 0.73$ , the Hubble parameter  $h = 0.7$ , the normalization of the Power spectrum  $n = 0.95$  and the amplitude of mass density fluctuation (at redshift  $z=0$ )  $\sigma_8 = 0.82$ . The number of particles used for each of the DM component was  $2048^3$ , resulting in a mass resolution of  $1.35 \times 10^8 M_{\odot} h^{-1}$ . Klypin et al. (2011).

The ranges of circular velocities for the host and subhalos and the corresponding number of halos at every redshift are listed in Table 1.

## 3. BULLET GEOMETRY AND MEASUREMENT SETUP

The configuration of the BGs in the simulations is shown in Figure 1. There we depict a host and its most massive sub-halo from in a particular case found at  $z=0$ . The arrows show the position and the velocity vectors sub-halo in a frame of reference where the main halo is at rest; thus  $\vec{v} = \vec{v}_{sub} - \vec{v}_{halo}$  and  $\vec{r} = \vec{r}_{sub} - \vec{r}_{halo}$ . The

Sample	Minimum $V_c$ km s $^{-1}$	Maximum $V_c$ km s $^{-1}$	# Halos $z = 0$	# Halos $z = 0.25$	# Halos $z = 0.5$	# Halos $z = 1$
Host	300	XX	400	362	310	192
Sub-structure	75	XX	XX	XX	XX	XX

TABLE 1  
CIRCULAR VELOCITY RANGES FOR THE HALOS AND SUBHALOS AT DIFFERENT REDSHIFTS.

angle between these two vectors characterized by,

$$\mu \equiv \cos(\theta) = \frac{\vec{v} \cdot \vec{r}}{\|\vec{v}\| \|\vec{r}\|} \quad (1)$$

encodes the geometry of the collision, i.e. cases of  $|\mu| \approx 1$  can be considered as head-on collisions while  $|\mu| \approx 0$  describe a grazing trajectory.

The bullet-like encounter can be instantaneously described by quantities the following quantities the circular velocity of the host and the sub-halo,  $V_{c,\text{host}}$  and  $V_{c,\text{sub}}$ ; the size of the host halo  $R_{\text{vir}}$ ; the relative position and velocity of the substructure,  $\vec{v}$  and  $\vec{r}$ ; and the angle between the position and velocity  $\mu$ .

As a first approximation there are two quantities that are available from observations of these Bullet-like systems. The projected distance between two dominant dark matter clumps and the ratio of the galaxies' luminosities associated to them. From the simulation point of view this can be translated into the 2D projected values of  $\|\vec{r}\|$ , its value relative to the virial radius  $X_{2D} = \|\vec{r}\|_{2D}/R_{\text{vir}}$  and the ratio of the circular velocities of the two clumps  $V_{c,\text{sub}}/V_{c,\text{host}}$ . In a higher degree of detail, in order to gain better insight we use the sub-structure velocity as a fraction of the host's circular velocity,  $\|\vec{v}\|/V_{c,\text{host}}$ , as a measure of the the strength of the interaction. Finally, we also measure the geometry of each interaction through the values for  $\mu$ .

All the physical quantities described above can be used to describe the three main stages in a bullet-like encounter. First, the sub-halo crosses the virial radius of the host halo starting a head on collision,  $\|\vec{r}\|/R_{\text{vir}} \approx 1$  and  $\mu \approx 0.0$ . Second, as the sub-halo crosses for the first time the center of the host halo  $\|\vec{r}\|/R_{\text{vir}} < 1.0$  and  $\mu > 0.0$ . Third, as the sub-halo reaches apogee and comes back to the center of the halo  $\|\vec{r}\|/R_{\text{vir}} < 1.0$  and  $\mu < 0.0$ . We use these quantities in Section XXX to fully characterize the different kind of interactions observed in the Bolshoi simulation.

#### 4. RESULTS

##### 4.1. Displacements and Relative Circular Velocities

The main result of this paper is summarized in Figure 2, it presents the integrated probability distribution for the displacement between the center of the host halo and its dominant sub-halo. The left panel shows the displacement in physical units and the right panel as a fraction of the virial radius of the host halo.

Figure 2 shows the results for two different populations; groups with  $300 \text{ km s}^{-1} < V_{c,\text{host}} < 700 \text{ km s}^{-1}$  and clusters with  $V_{c,\text{host}} > 700 \text{ km s}^{-1}$ . Additionally, this is presented for all redshifts  $z = 0.0, 0.25, 0.5$  and  $1.0$ .

The panel with the physical displacements also shows a vertical stripe with the estimated displacement for the

Bullet-group reported by Gastaldello et al. (2014). Considering this system as consistent with the groups sample we see that a fraction of  $\sim XX \pm XX\%$  of the groups should present a displacement equal or larger than the one estimated for SL2S J08544-0121. The panel with the normalized displacements shows a distribution that can be considered close to universal in the sense that the two samples (groups and clusters) at all redshifts present a similar trend. [...]

Figure 3 shows 2D histograms in a plane composed by the ratio of the two circular velocities  $V_{c,\text{sub}}/V_{c,\text{host}}$  and the physical displacements. In each of the halo samples (left, groups; right, clusters) the two-dimensional distributions are similar and have been therefore integrated to build the 2D histogram.

On top of these 2D histograms there is a circle with error bars that represents the observational estimates for the system SL2S J08544-0121. [...]

##### 4.2. Relative Velocities

In Figure 4 we present the integrated probability of the relative peculiar velocities of the sub-halos with respect to the host halo. The left panel presents this velocity in physical units while the left panel presents them as a fraction of the circular velocity of the host halo.

##### 4.3. Collision Geometries

##### 5. DISCUSSION

Strictly speaking our results apply to multimodal groups and the expected separation between dark matter clumps. [...]

Expected displacement between dark and baryonic components are better described by systems where the collision already occurred. [...] (comparison with the old bullet clusters paper?)

The expectations to quantify this effects observationally are high. [...]

In order to facilitate the reproducibility and reuse of our results we have made available all the data and the source code available in a public repository. [...]

##### 6. CONCLUSIONS

We selected four snapshot of the simulation for four different redshifts ( $z = 0, z = 0.25, z = 0.5$  and  $z = 1$ ) based in the distribution of redshift in the Figure 1 by Verdugo & Foex (2014), and for each sample in redshift we selected the host halo with circular velocities greater than  $300 \text{ km s}^{-1}$  and was split in two principal groups: The first group correspond to host halo with circular velocities between  $300 \text{ km s}^{-1}$  to  $700 \text{ km s}^{-1}$  with mass in the range of  $10^{12} M_{\odot}$  to  $10^{14} M_{\odot}$  in the range of mass of the Bullet Groups, and second group correspond to host halo with circular velocities greater than  $700 \text{ km s}^{-1}$  with mass  $\geq 10^{14} M_{\odot}$ , in the range of mass of the Bullet Clusters, in the Table 1 is shown the two groups selected in this

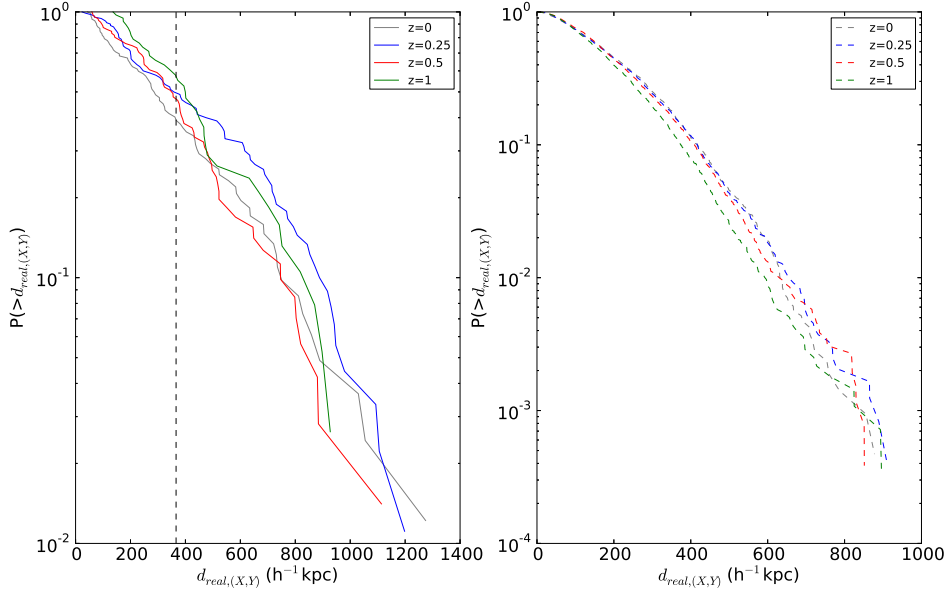


FIG. 2.— Integrated probability distribution for the displacement between the host halo and its dominand sub-halo. The left panel shows the results in terms of the physical displacements and the right panel the same displacement normalized by the virial radius of the host halo. The continuous line corresponds to the halos in the group sample  $V_{c,\text{host}} > 700 \text{ km s}^{-1}$  and the dashed lines to the The vertical stripe corresponds to the estimate of the separation between the two dark matter clumps in the results reported by Gastaldello et al. (2014) for the group SL2S J08544-0121. The right panel shows the same results normalized by the virial radius of the host halo.

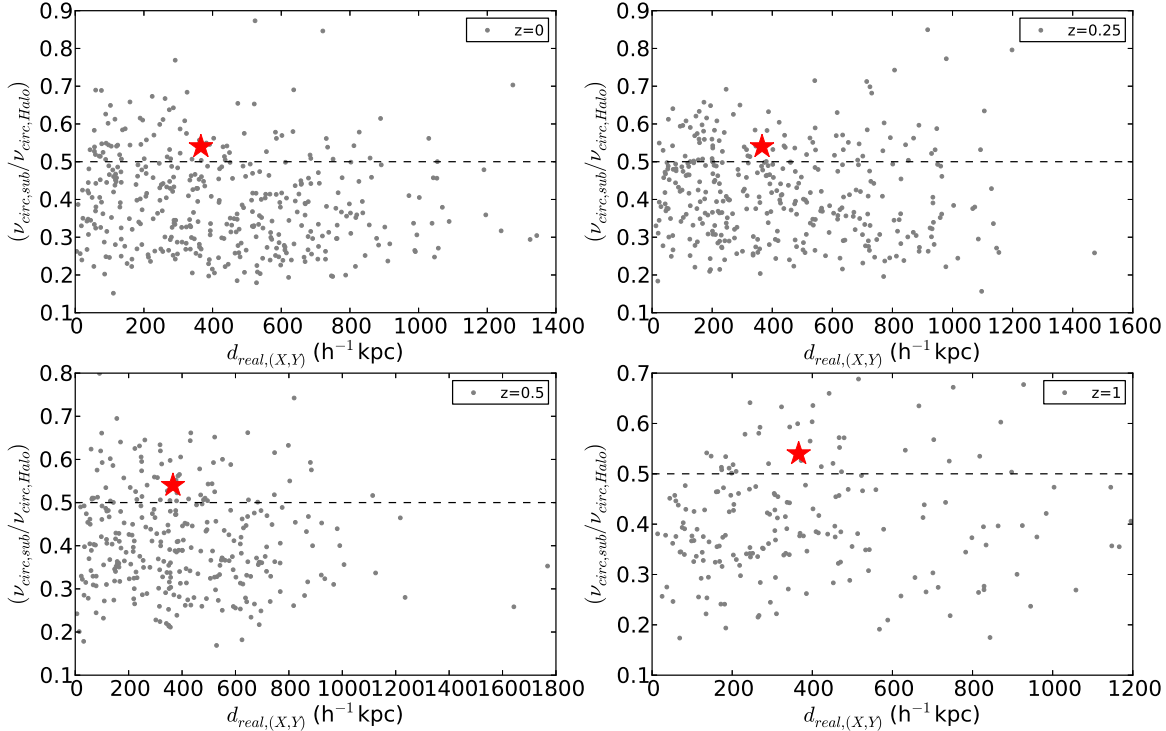


FIG. 3.— 2D histogram in the plane  $V_{c,\text{sub}}/V_{c,\text{host}} - d_{2D}$ . The left panel corresponds to groups and the right panel to clusters. The circle with error bars corresponds to SL2S J08544-0121 data reported from Muñoz et al. (2013) and Gastaldello et al. (2014). The data used to construct the histograms integrates the objects at all redshifts.

FIG. 4.— Integrated probability distribution for the relative velocity of the sub-halo with respect to its host. The left panel shows the results in physical units while the right panel show the same values normalized by the circular velocity of the host halo. The line coding follows the same structure as Figure ??

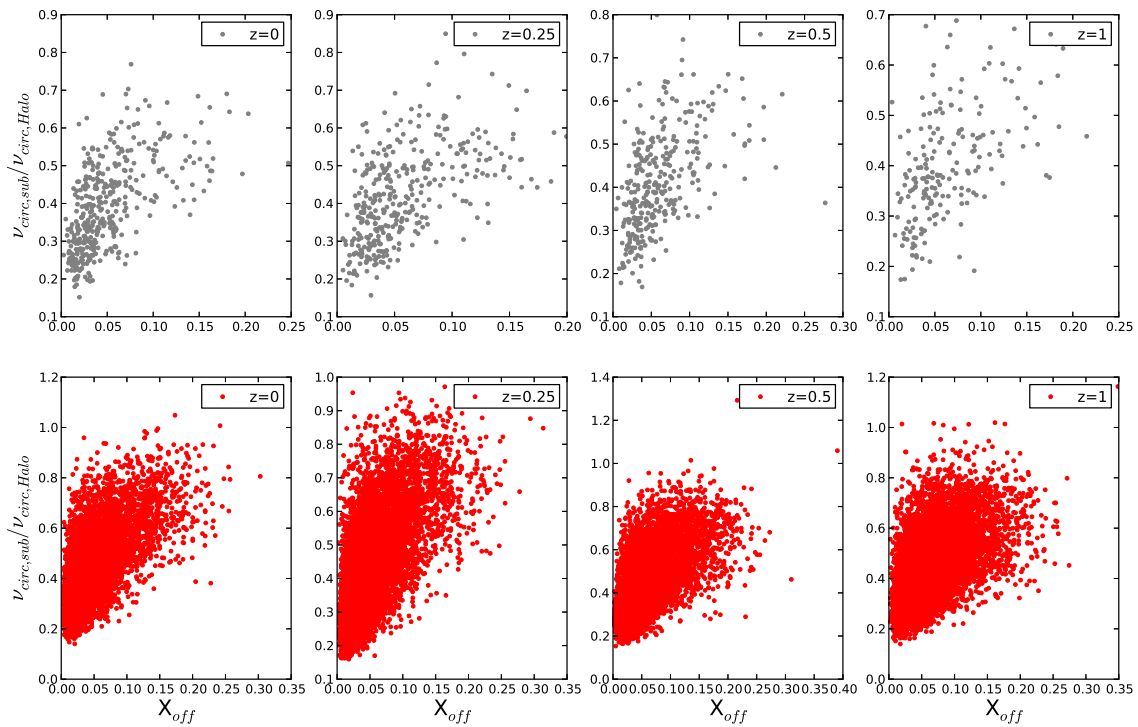


FIG. 5.— Scatter plot for  $X_{off}$  as function of the relation between velocities of substructures and the host halos and for different  $z$ . The top panel is represented to the sample with  $v > 700 \text{ km s}^{-1}$  and down panel is represented for  $v < 700 \text{ km s}^{-1}$

FIG. 6.— Integrated distributions of  $|\vec{v}|/V_{c,\text{host}}$  at all  $z$ . The left panel correponds to the sample with  $V_{c,\text{host}} > 700 \text{ km s}^{-1}$  and right panel correpond to the sample with  $V_{c,\text{host}} < 700 \text{ km s}^{-1}$ .

work. For each group, we classified the corresponding substructures most massive and associated with the corresponding host halo. In this work, we estimate the expected distribution of displacements ( $d_{real,(X,Y)}$ ) in the projection 2-D that can be estimated by observations, these displacements correspond to the separation between the minimal potential of the host halo and the minimal potential of the substructure, both are dark matter distributions.

In order to explore the distribution of displacements expected in the observational, we define a new parameter given by:

$$\frac{v_{circ,sub}}{v_{circ,halo}} = 0.5 \quad (2)$$

Figure ?? shows the scatter plot of the parameter  $\left(\frac{v_{circ,sub}}{v_{circ,halo}}\right)$  vs the displacement ( $d_{2d,(X,Y)}$ ) between the host halo and the substructure and for different redshifts. This parameter is consistent with the observations. The red star symbol in the Figure ?? is equal to 0.54 corresponding to the fraction in velocity dispersion in the line-of-sight of the group SL2S SJ08544-0121 ( $\sigma_{host,halo} = 341^{+43}_{-109}$  kms $^{-1}$  and  $\sigma_{substructure} = 185^{+30}_{-62}$ ), reported by Muñoz et al. (2013). Based in the parameter

$\left(\frac{v_{circ,sub}}{v_{circ,halo}}\right) > 0.5$ , we estimate the expected distribution of displacements and this is shown in the Figure ?? for the two groups classified in this work.

### 6.1. Number expected of Bullet Groups in the sample

In order to estimate the number of Bullet Groups expected in the Bolshoi Cosmological Simulation, we define the configuration of this system as one where the substructure is coming out of the host halo ( $\cos(\theta) > 0.5$ ). For this we make the scalar product between the velocity vector and position vector that defines the separation between the host halo and the substructure, as shown below:

## 7. DISCUSSION

## 8. CONCLUSIONS

## ACKNOWLEDGEMENTS

The CosmoSim database used in this paper is a service by the Leibniz-Institute for Astrophysics Potsdam (AIP). The BolshoiP simulation was performed within the Bolshoi project of the University of California High-Performance AstroComputing Center (UC-HIPACC) and was run at the NASA Ames Research Center.

## REFERENCES

- Gastaldello, F., Limousin, M., & Foex, G. 2014, MNRAS submitted  
 Klypin, A. A., Trujillo-Gomez, S., & Primack, J. 2011, ApJ, 740, 102  
 Muñoz, R. P., Motta, V., Verdugo, T., Garrido, F., Limousin, M., Padilla, N., Foëx, G., Cabanac, R., Gavazzi, R., Barrientos, L. F., & Richard, J. 2013, A&A, 552, A80  
 Verdugo, T., & Foex, G. 2014, å submitted

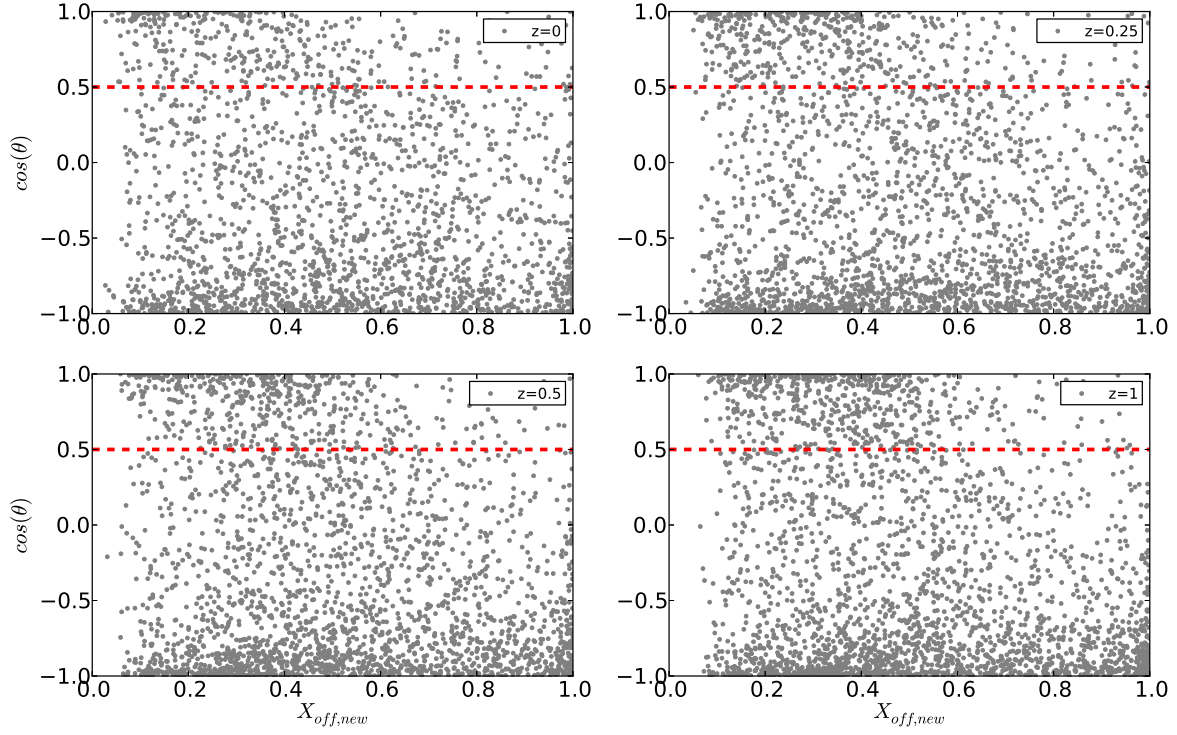


FIG. 7.— Scatter of  $\cos(\theta)$  vs  $X_{off,new}$ . The red dashed line correpond to the limit for  $\cos(\theta) > 0.5$ , where the substructure is emerging from the host halo and  $\left(\frac{v_{circ,sub}}{v_{circ,halo}}\right) \geq 0.5$ , circular velocities  $< 700 \text{ kms}^{-1}$  and different redshifts.

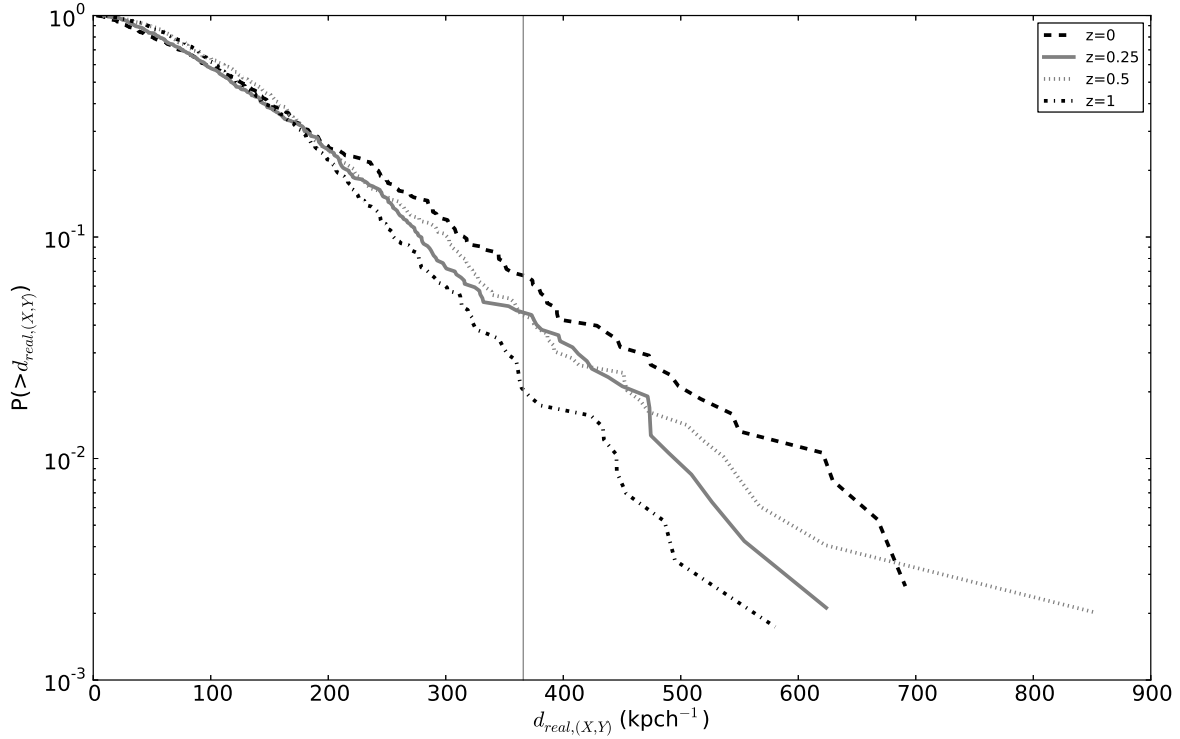


FIG. 8.— Cumulative distribution of  $d_{real,(X,Y)}$  for  $\cos(\theta) > 0.5$ ,  $\left(\frac{v_{circ,sub}}{v_{circ,halo}}\right) \geq 0.5$ , circular velocities  $< 700$  kms $^{-1}$  and different redshifts.